

REAL FLUID MODELLING OF SUPERCRITICAL REACTING FLOWS IN LIQUID ROCKET ENGINE

Maria Grazia De Giorgi, and Antonio Ficarella

University of Salento –Dep. Engineering for Innovation , Lecce, Italy, I-73100

Abstract

A current problem is to understand the injection, mixing and combustion in typical liquid rocket engines at combustion chambers conditions. Until now, only H₂/LO_x injection and combustion has been investigated deeply, while there is a lack in experimental data and numerical studies in literature on LO_x/CH₄ combustion, and it is not possible to transfer concepts design from LOX/H₂ injector to LO_x/CH₄ injector. At typical injection conditions H₂ is far in the supercritical region and shows in a good approximation ideal gas behavior. Methane however is near critical and real gas effects are to be taking into account in the mixing process. The prediction of all thermodynamic properties depend on the equation of state chosen. In the present work CFD simulations have been performed for the simulation of supercritical LO_x- CH₄ spray using the Soave-Redlich-Kwong and the Peng Robinson equations of state.

Nomenclature

ρ	pressure
R	gas constant
T	temperature
V	specific volume
v	molar volume
ω	acentric factor
H	enthalpy
C_p	isobaric specific heat
Z	compressibility factor
C_v	isochoric heat capacity
S	entropy
μ	dynamic viscosity
M_w	molecular weight
k	thermal conductivity
Y_i	mass fraction of species i

Superscripts

R	real gas property
(0)	reference state

Subscripts

c	value at critical point
r	reduced value

1. INTRODUCTION

The necessity to enhance the performance of high-pressure combustion devices in liquid-propellant rockets requires high chamber pressures. In a liquid rocket engine thrust chamber, higher chamber pressures allow a higher specific impulse for the engine to be produced. Higher chamber pressures similarly increase the power output and efficiency of gas turbines and diesel engines. This has motivated a general trend towards increasingly higher chamber pressures in propulsion applications. Liquid fuels and/or oxidizers are usually delivered to combustion chambers as a spray of droplets, which then undergo a sequence of vaporization, mixing, ignition, and combustion processes at pressure levels well above the thermodynamic critical points of the fluid. Near the critical point, reactants properties show liquid-like densities, gas-like diffusivities, and pressure-dependent solubility.

In the past research [1–3] has concerned the cryogenic propellant combustion under subcritical and transcritical conditions, in particular in the case of liquid oxygen and gaseous hydrogen injected from a single element at various chamber pressures (0.1–7 MPa). Recently, there is a great interest in the development of reusable liquid rocket engines operating with methane and oxygen as propellants.

Extensive efforts have been made in experimental works to characterize the dynamics of supercritical fluid injection and mixing [4–8]. Observations of high-pressure liquid oxygen/hydrogen and liquid oxygen/ methane propellant injection under reacting conditions have shown significant physical disparities between sub-, trans- and supercritical injection and atomisation regimes. This has due to the strong thermodynamic gradients and non-idealities experienced under near critical, transcritical and supercritical pressure conditions.

However exhaustive experimental testing of liquid rocket engines at representative operating conditions is prohibitively expensive and will eventually be replaced or at least reduced by advanced numerical modeling. So in parallel to experimental studies, attempts were made both theoretically and numerically to explore the underlying mechanisms of high-pressure fluid injection and mixing [9–11]. Numerical modeling of supercritical mixing and combustion processes is very complex, it poses a variety of challenges due to the introduction of thermodynamic non-idealities and transport anomalies. In addition to the classical closure problems associated with turbulent reacting flows, the situation is compounded with increasing pressure due to the introduction of thermodynamic non idealities and transport anomalies. Such thermodynamic non-idealities warrant the evaluation of real fluid properties when considering supercritical or near critical conditions.

The prediction of all thermodynamic properties depend on the equation of state chosen. Thus, appropriate equations of state (EOS), and methods to determine transport properties must be provided. Few works in literature deal with the reacting flows taking into account real gas effects. In the present work CFD simulations have been performed for the simulation of supercritical LOx- CH₄ spray, without and with reactions: External routines have been implemented in the code Fluent to model the physical properties of the species in the single step methane/oxygen reacting mixture, by the real gas model, using the Soave-Redlich-Kwong and the Peng Robinson equations of state, to compare the two approaches. An E.D.M. model describes the turbulence-chemical kinetics coupling.

2. EQUATION OF STATE AND THERMODYNAMIC PROPERTIES

Considering the continuous variations of fluid properties in supercritical environments, classical techniques dealing with liquids and gases individually lead to erroneous results.

In this section a theoretical study has been done to clarify the great importance of real gas effects in the calculation of species properties at supercritical pressure, typical of liquid rocket engine.

There are a lot of equation of state for real gas available in literature, from the simplest to the most complicated; nevertheless there is the necessity to understand which equation could tackle better mixing and combustion phenomena modeling in the typical liquid rocket engine operating ranges.

In this work a comparison among two of the most common real gas equations of state at conditions of interest is presented. These equations are the SRK (Soave-Redlich-Kwong), and the PR (Peng-Robinson) equation of state. These equations have been chosen because they are linear and cubic, therefore they are simple to solve and to implement in a CFD code.

2.1 The Soave-Redlich-Kwong (SRK) equation of state

The Soave-Redlich-Kwong (SRK) equation of state takes the form:

$$p = \frac{RT}{(V - \bar{b})} - \frac{a(T)}{V(V + b_0)} \quad (1)$$

Where R is the universal gas constant. The parameters, a and \bar{b} , accounting for the effects of attractive (a) and repulsive forces (\bar{b}) among molecules, respectively, are calculated using the following equation:

$$\begin{aligned} a(T) &= a_0 \left(\frac{T_c}{T}\right)^n & a_0 &= 0.42747 \frac{R^2 T_c^2}{p_c} & b_0 &= 0.08664 \frac{RT_c}{p_c} \\ c_0 &= \frac{RT_c}{p_c + \frac{a_0}{V_c(V_c + b_0)}} + b_0 - V_c & \bar{b} &= b_0 - c_0 \end{aligned} \quad (2)$$

Where T_c and p_c are the critical temperature and pressure. The value of the exponent n , in the function $a(T)$ will depend on the substance; values of n are well correlated by the empirical equation [12]:

$$n = 0.4986 + 1.1735\omega + 0.475\omega^2 \quad \text{and} \quad \omega = \log\left(\frac{p_v}{p_c}\right) - 1 \quad (3)$$

where ω is the acentric factor and p_v is the saturated vapor pressure evaluated at temperature $T = 0.7T_c$.

To compute the density the SRK equation must be solved for the specific volume; for convenience, it can be written as a cubic equation for specific volume:

$$V^3 + a_1 V^2 + a_2 V + a_3 = 0 \quad (4)$$

where

$$a_1 = c_0 - \frac{RT}{p} \quad a_2 = -\left(\bar{b}b_0 + \frac{RTb_0}{p} - \frac{a(T)}{p}\right) \quad a_3 = -\frac{a(T)\bar{b}}{p} \quad (5)$$

Eq. (4) is solved with a standard algorithm for cubic equations [13]; the derivatives of specific volume with respect to temperature and pressure can be easily determined from Eq. (1) using implicit differentiation. The results are:

$$\left(\frac{\partial V}{\partial p}\right)_T = -\frac{(a_1)'_p V^2 + (a_2)'_p V + (a_3)'_p}{3V^2 + 2a_1 V + a_2} \quad (6)$$

$$\left(\frac{\partial V}{\partial T}\right)_p = -\frac{(a_1)'_T V^2 + (a_2)'_T V + (a_3)'_T}{3V^2 + 2a_1 V + a_2} \quad (7)$$

where

$$(a_1)'_p = \frac{RT}{p^2}, \quad (a_2)'_p = \frac{RTb_0 - a(T)}{p^2}, \quad (a_3)'_p = \frac{a(T)\bar{b}}{p^2}$$

$$(a_1)'_T = -\frac{R}{p}, \quad (a_2)'_T = \frac{-Rb_0 + \frac{da(T)}{dT}}{p}, \quad (a_3)'_T = -\frac{da(T)\bar{b}}{dT p} \quad \frac{da(T)}{dT} = -n \frac{a(T)}{T} \quad (8)$$

Enthalpy for a real gas can be written

$$H = H^0(T) + pV - RT - \frac{a(T)}{b_0} (1+n) \ln\left(\frac{V+b_0}{V}\right) \quad (9)$$

In the present case a fourth-order polynomial for the specific heat for a thermally perfect gas [14] has been used:

$$C_p^0(T) = C_1 T^{-2} + C_2 T^{-1} + C_3 + C_4 T + C_5 T^2 + C_6 T^3 + C_7 T^4 \quad (10)$$

The specific heat for the real gas can be obtained by differentiating Eq. (9) with respect to temperature (at constant pressure):

$$C_p = \left(\frac{\partial H}{\partial T}\right)_p \quad (11)$$

The result is:

$$C_p = C_p^0(T) + p \left(\frac{\partial V}{\partial T}\right)_p - R - \frac{da(T)}{dT} \frac{(1+n)}{b_0} \ln\left(\frac{V+b_0}{V}\right) + a(T)(1+n) \frac{\left(\frac{\partial V}{\partial T}\right)_p}{V(V+b_0)} \quad (12)$$

2.2 The Peng-Robinson (PR) Equation of State

The Peng-Robinson equation of state is one of the most frequently used cubic equations of state because its implementation is straightforward and it is more accurate than other equation of state. The general form of this equation is:

$$p = \frac{RT}{(v - \bar{b})} - \frac{a(T)}{v(v + b) + b(v - b)} \quad (13)$$

where R is the universal gas constant and v is the molar volume. The parameter a and b account for the effects of attractive and repulsive forces between the molecules, given by:

$$a(T) = a \left[1 + m \left[1 - \sqrt{T/T_c}\right]\right]^2 \quad a = 0.45723553 \frac{R^2 T_c^2}{p_c} \quad b = 0.077796074 \frac{RT_c}{p_c}$$

$$m = 0.37464 + 1.54226\omega - 0.26992\omega^2 \quad (14)$$

Where T_c and p_c are the critical temperature and pressure and ω is the acentric factor defined in the previous section.

The Peng-Robinson equation of state has been solved using this procedure [15] :to compute the density the PR equation must be solved for the specific volume; for convenience, it can be written as a cubic equation for molar volume:

$$v^3 + a_1 v^2 + a_2 v + a_3 = 0 \quad (15)$$

where

$$a_1 = b - \frac{RT}{p} \quad a_2 = -\left(3b^2 + \frac{2RTb}{p} - \frac{a(T)}{p}\right) \quad a_3 = \frac{b^2RT}{p} - b^3 - \frac{a(T)b}{p} \quad (16)$$

Eq. (15) is solved with a standard algorithm for cubic equations [16]; to calculate isobaric specific heat we must calculate $(\partial p/\partial v)_T$, $(\partial T/\partial p)_v$ and $(\partial v/\partial T)_p$ derivatives. For convenience the PR equation is often written in a cubic polynomial form for the compressibility factor Z:

$$f(Z) = Z^3 + \alpha Z^2 + \beta Z + \gamma = 0 \quad (17)$$

where

$$\alpha = B - 1 \quad \beta = A - 2B - 3B^2 \quad \gamma = B^3 + B^2 - AB \quad A = a(T)p/(RT)^2 \quad B = bp/RT \quad (18)$$

This approach is valid only for a pure component, not mixture. With knowledge of the molar volume and compressibility, the three PVT derivatives can be calculated. Knowledge of these quantities is prerequisite to finding most any derivative thermodynamic property. These three derivatives must satisfy the “cyclical rule”, which may be written as

$$\left(\frac{\partial p}{\partial v}\right)_T \left(\frac{\partial T}{\partial p}\right)_v \left(\frac{\partial v}{\partial T}\right)_p = -1 \quad (19)$$

Therefore, once we have values for any two of the three PVT derivatives, the third may be calculated from Eq. (19). The first derivative in Eq. (19) is found by direct differentiation of Eq. (13):

$$\left(\frac{\partial p}{\partial v}\right)_T = \frac{-RT}{(v-b)^2} + \frac{2a(T)(v+b)}{[v(v+b)+b(v-b)]^2} \quad (20)$$

The second derivative in Eq.(19) is also found by direct differentiation of Eq.(13):

$$\left(\frac{\partial p}{\partial T}\right)_v = \frac{R}{(v-b)} - \frac{a'(T)}{v(v+b)+b(v-b)} \quad (21)$$

where

$$a'(T) = \frac{da(T)}{dT} = \frac{-ma(T)}{[1+m(1-\sqrt{T/T_c})]\sqrt{TT_c}} \quad (22)$$

To compute isobaric heat capacity we have to calculate the isochoric heat capacity for a real gas, given by Walas [16], Carnahan [17] and Kyle [18]:

$$C_v^R = \frac{Ta''(T)}{b\sqrt{8}} \ln \left(\frac{Z+B(1+\sqrt{2})}{Z+B(1-\sqrt{2})} \right) \quad (23)$$

where

$$a''(T) = \frac{d^2a(T)}{dT^2} = \frac{am(1+m)\sqrt{\frac{T_c}{T}}}{2TT_c} \quad (24)$$

Then isobaric specific heat will be given by the sum of the ideal and real contributions:

$$C_p = C_p^{ID} + C_p^R \quad (25)$$

From the general relationship between C_v and C_p we have at the end:

$$C_p^R = C_v^R + T \left(\frac{\partial p}{\partial T} \right)_v \left(\frac{\partial v}{\partial T} \right)_p - R \quad (26)$$

Figure 1 show comparisons of predicted density using Ideal Gas , SRK and PR equations with the experimental tabulated data for methane and oxygen at constant pressure value, equal to 15 MPa. National Institute of Standards and Technology (NIST) tables provide experimental data for density and isobaric heat capacity [19-20]. It is noticed that disparity between prediction using real gas equation (SRK and PR) and experiments is negligible. Even in the critical region, the error, with respect to the NIST data, does not exceed 5 % in the PR and 2 % in the SRK equations of state, while the error reaches the 50% for the ideal gas equation.

The comparison with ideal-gas and experimental data for the isobaric specific heat still underline the necessity to use the real gas equation instead an ideal gas approach, the both the real gas equation equations of state , SRK and PR, well predict the real gas properties at higher temperatures, near the critical point the best performance are for the PR equation. So the PR equation is preferable in the cold flow simulations, while the SRK and PR will give similar results at higher temperatures, as in reacting flow.

3. CFD MODELING

Numerical simulations have been done implementing real gas models by user defined routines in the CFD code Ansys Fluent v.12.0. The test case is a methane-oxygen coaxial liquid rocket injector at supercritical and transcritical conditions . Oxygen is injected from a central duct while methane enters the chamber from an annular coaxial duct. Figure 3 shows the computational domain, a two-dimensional structured axisymmetric grid with 160000 cells has been used. The diameter of the central duct is equal to 0.007 m, while the external diameter of the annular coaxial duct is 0.01 m, the O₂ post tip thickness is 0.0004 m.

Different fluid operating conditions have been studied, comparing different modelling approaches for the species properties. Supercritical cold flow injection have been simulated, at methane and oxygen inlet temperature set to 300K, for oxygen inlet velocity $V_{O_2} = 20$ m/s, and three different methane inlet velocity ($V_{CH_4} = 70$ m/s in the case 1, $V_{CH_4} = 100$ m/s in the case 2 and $V_{CH_4} = 115$ m/s in the case 3). Then trans-critical cold flow injection (case 4) has been analyzed assuming: oxygen inlet velocity $V_{O_2} = 10$ m/s; methane inlet velocity $V_{CH_4} = 93$ m/s, for oxygen temperature $T_{O_2} = 100$ K and methane temperature $T_{CH_4} = 300$ K.

Finally the case 1 has been studied also under combustion conditions (case 5), assuming inlet oxygen and methane temperature $T_{O_2} = T_{CH_4} = 300$ K, oxygen inlet velocity $V_{O_2} = 20$ m/s; methane inlet velocity $V_{CH_4} = 70$ m/s. In this case only the SRK real gas model has been used because the properties predicted by the SRK and the PR real gas model are quite similar at high temperature as shown in figure 1 and figure 2. The NIST database has been not used because the range of applicability is limit to temperature lower than 625 K for methane and 1000 K for oxygen. For each case the chamber pressure has been assumed equal to 150 bar, a typical value for booster or main stage liquid rocket engine [21].

The CFD code used in the present study models mixing and transport of chemical species by solving conservation equations describing convection, diffusion, and reaction sources for each component species. Multiple simultaneous chemical reactions can be modelled, with reactions occurring in the bulk phase (volumetric reactions) and/or on wall or particle surfaces, and in the porous region.

The modelling of species transport and reactions has been done using the Eddy Dissipation Model (EDM) in the CFD code. In this model reaction rates are assumed to be controlled by the turbulence, so expensive Arrhenius chemical kinetic calculations can be avoided. The model is computationally cheap, but, for realistic results, only one or two step heat-release mechanisms should be used. In the simulations $\kappa - \epsilon$ turbulence models has been used.

External routines have been implemented in the code to model the physical properties of the species in the single step methane/oxygen reacting mixture, definition of functions of the Soave-Redlich-Kwong (SRK) and Peng Robinson (PR) real gas model for the individual species property calculations and functions for the mixture properties, computed assuming ideal gas mixing rule.

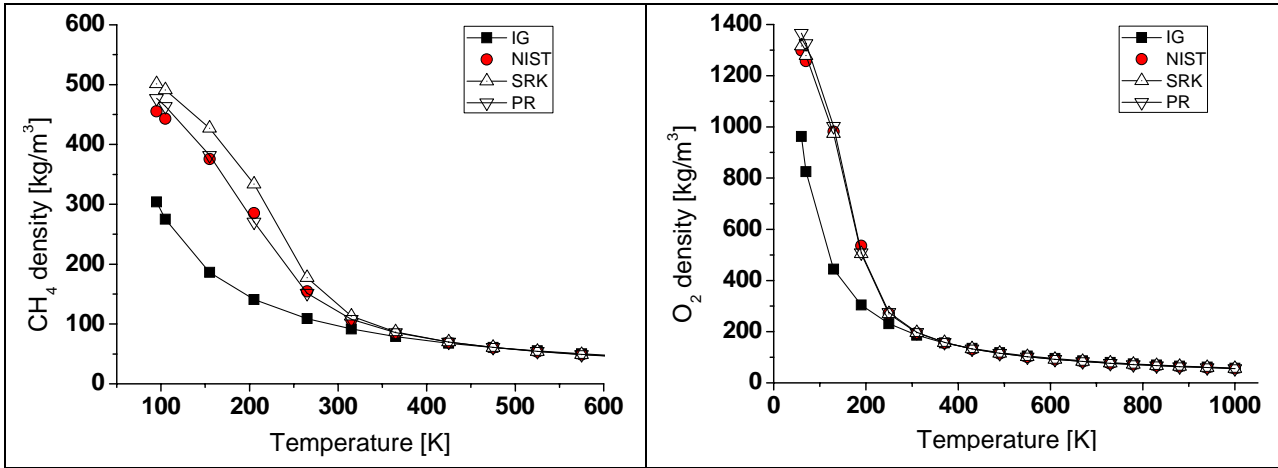


Figure 1 - CH₄ and O₂ density comparison at 15 MPa.

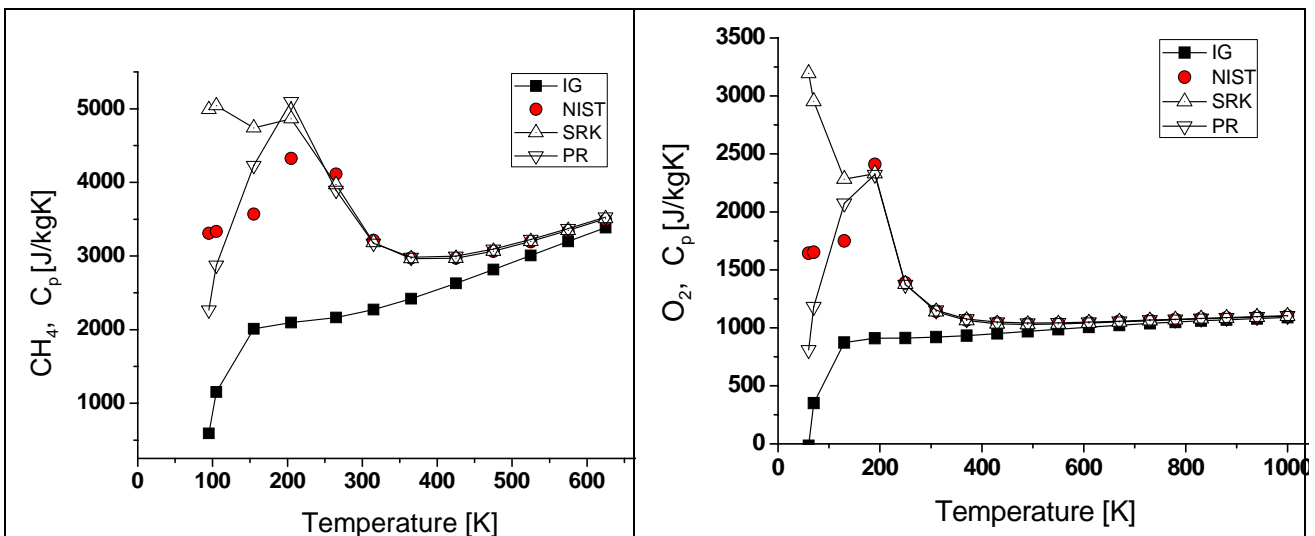


Figure 2 - CH₄ and O₂ isobaric specific heat comparison at 15 MPa.

4. Results and discussion

4.1 Cold flow simulations

As explained in the previous section, cold flow simulations have been performed by different approaches for the modelling of species properties: assuming ideal gas, using the NIST database, jet implemented in Ansys Fluent 12.0 and finally using two different real gas models, the Soave-Redlich-Kwong (SRK) real gas model and Peng-Robinson (PR) real gas model. Figure 4 shows the computed mass fraction profiles, the ones, referring to a section very close to the injection point ($x/D = 0.3$), show the good agreement between real gas model predictions and ideal gas. Strong discrepancies exist between the ideal gas predictions and the real gas

models (SRK and PR) at highest distance from the nozzle exit ($x/D=5.0$) in the case 4, where temperature is supercritical for methane and sub-critical for oxygen. As shown in figure 6 the length of the potential core, defined as the axial position where the oxygen mass fraction is equal to 0.9, is higher for the ideal gas than the real gas models PR and SRK. For the supercritical cold injection (case 1-3) the predictions are quite similar between the different models, while discrepancies are evident in the transcritical case 4. In this case the difference between the real gas models results and the NIST database is evident. This can be due to the limitation of the NIST real gas model, implemented by default in the code, that assumes that the fluid you will be using in the computation is superheated vapor, supercritical fluid, or liquid. The different behaviour between computations with real gas model and that one with ideal gas is in agreement with the previous considerations about the species properties in figure 1 and figure 2, when it has been underlined the necessity to use the real gas equation instead an ideal gas approach near the critical point.

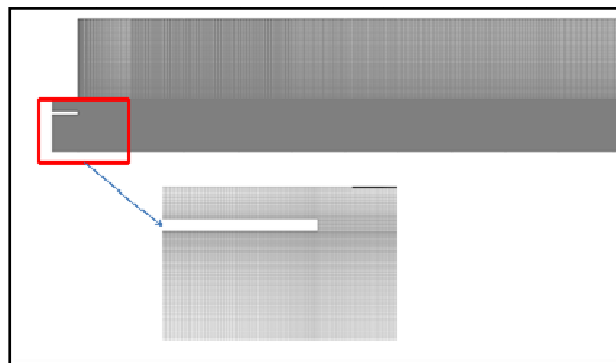


Figure 3 – Computational domain

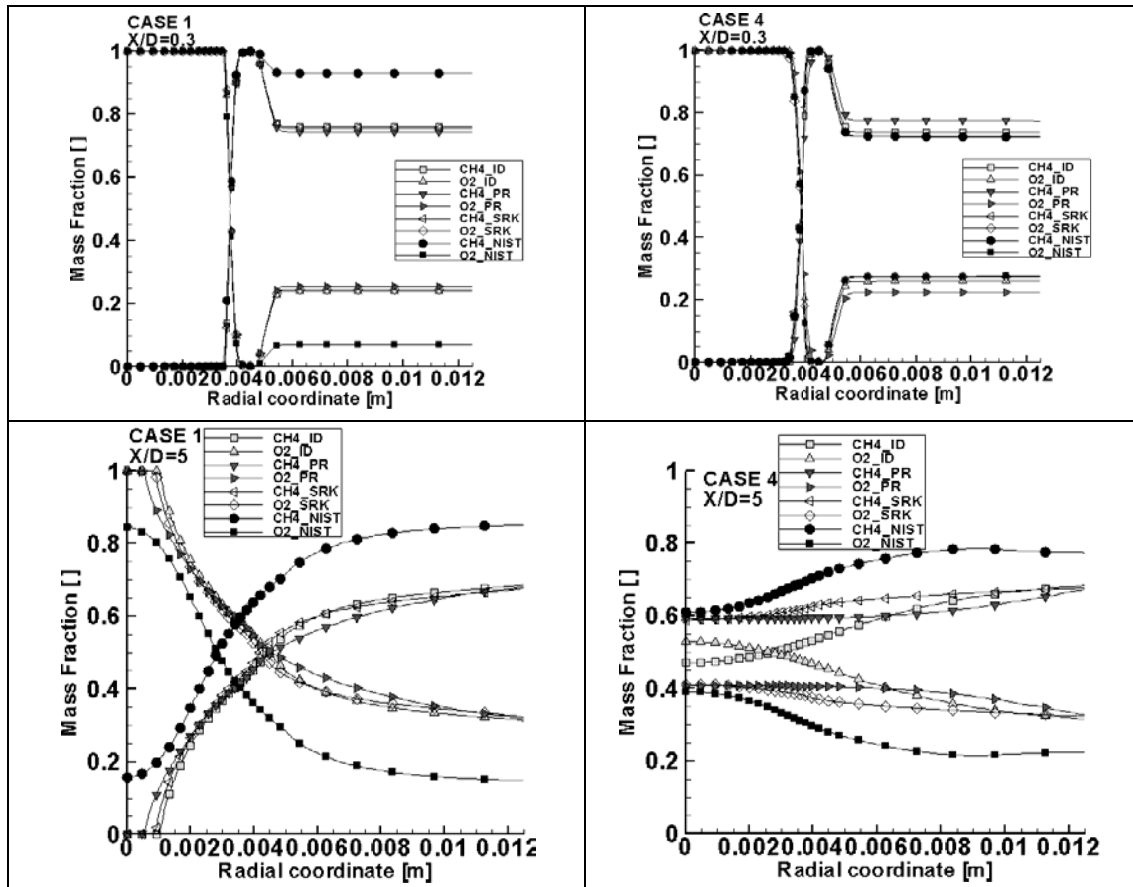


Figure 4 - Species radial profiles at $x/D=0.3$, and $x/D=5.0$ in the case 1 and case 4 simulation with Ideal Gas, PR and SRK equation of state and NIST data.

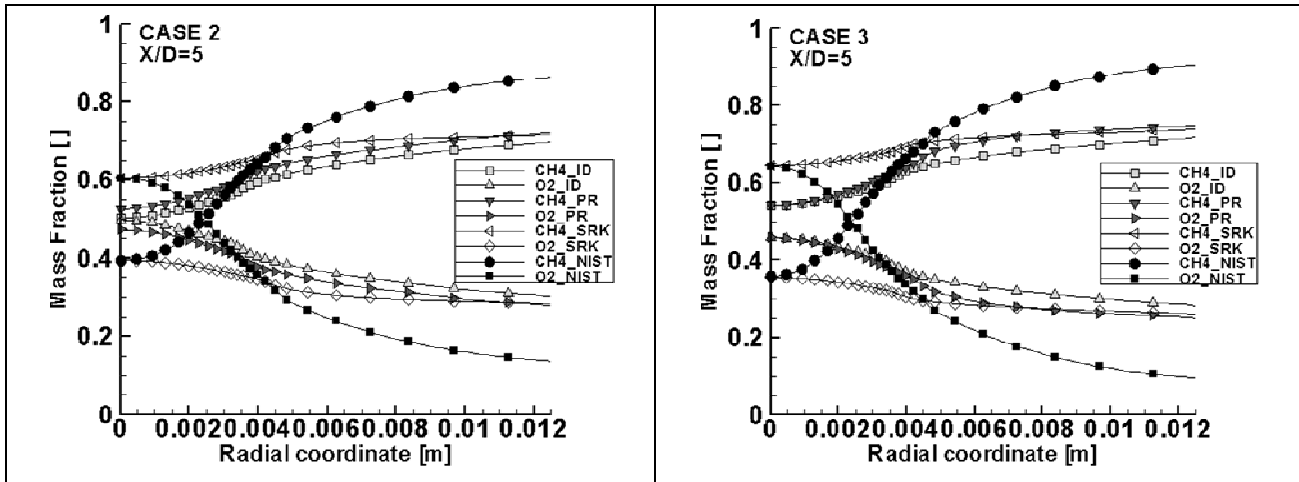


Figure 5 - Species radial profiles at $x/D=5.0$ in the case 2 and case 3, simulations with Ideal Gas, NIST, Peng Robinson (PR) and Soave-Redlich-Kwong (SRK) properties.

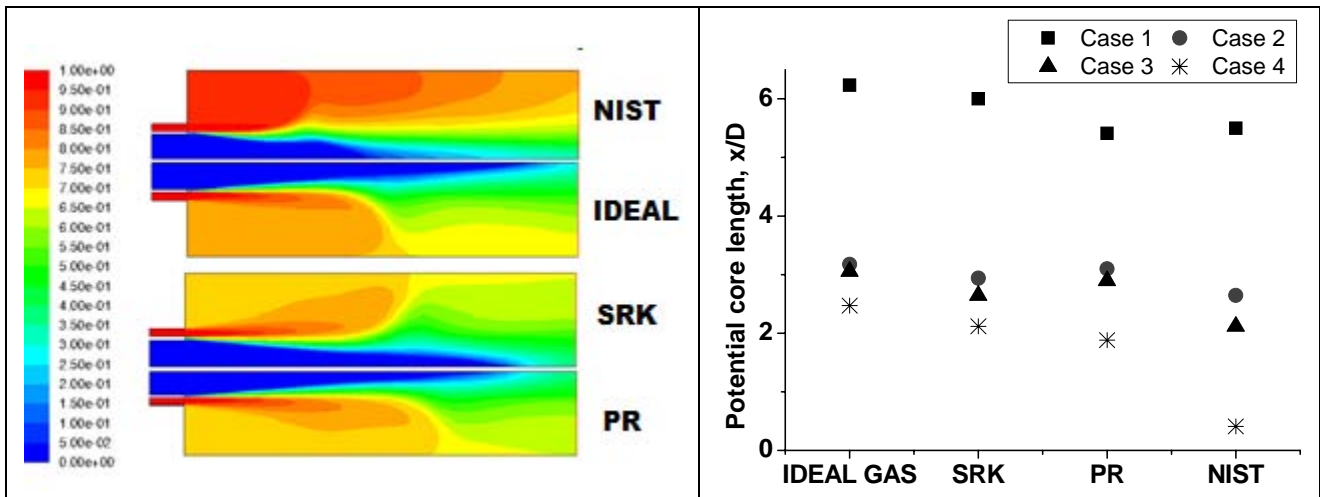


Figure 6 – On the left: methane mass fraction simulation with Ideal Gas, PR and SRK properties and NIST database (case1). On the right: potential core length predictions.

4.2 Reacting flow simulations

The reacting flow simulations have been done to study the typical methane-oxygen shear coaxial injector geometry under supercritical conditions, following a step-by-step procedure: first cold flow simulations, without reactions and combustion, are performed. Then, starting from a convergent cold flow solution, reactions can be activated: the eddy dissipation model (EDM) is used to compute the reacting flow. This model assume that chemical reactions are infinitely fast with a single step global mechanism (no production of radicals and intermediate species); even though this is a very crude model, in a real liquid rocket engine thrust chamber, due to the high pressure and temperature environment, chemical reactions take place at very small characteristic times, a suitable condition for a fast chemistry assumption.



The geometry of the test is that one used for the cold flow simulations.

In figure 7 the temperature, predicted by the ideal gas and the real gas SRK equation of state, are shown. The flame shape for ideal gas and SRK real gas equation of state is different, with a smaller region at high temperature in the case of ideal gas properties simulation. Qualitatively comparison with experimental studied on combustion of LOx/CH₄ spray present in literature [22], see figure 8, shows good agreement of the SRK predictions with the experimental flame shape. Finally in figure 9 the species radial profiles have been shown.

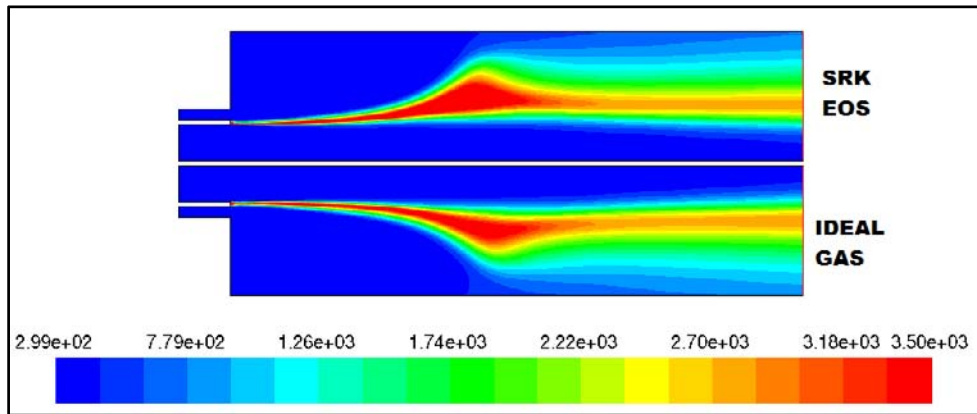


Figure 7 – Temperature field in the case 5 simulation with Ideal Gas and SRK properties.

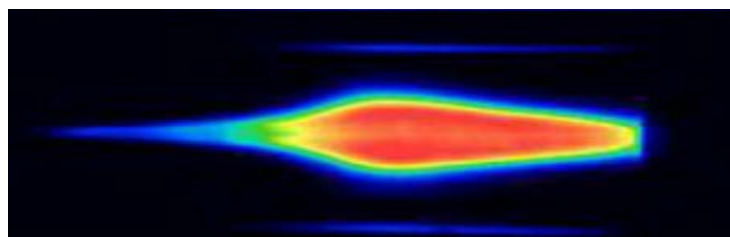


Figure 8 - Experimental observations of LOx/CH₄ flame by M. Oschwald et al. [22]

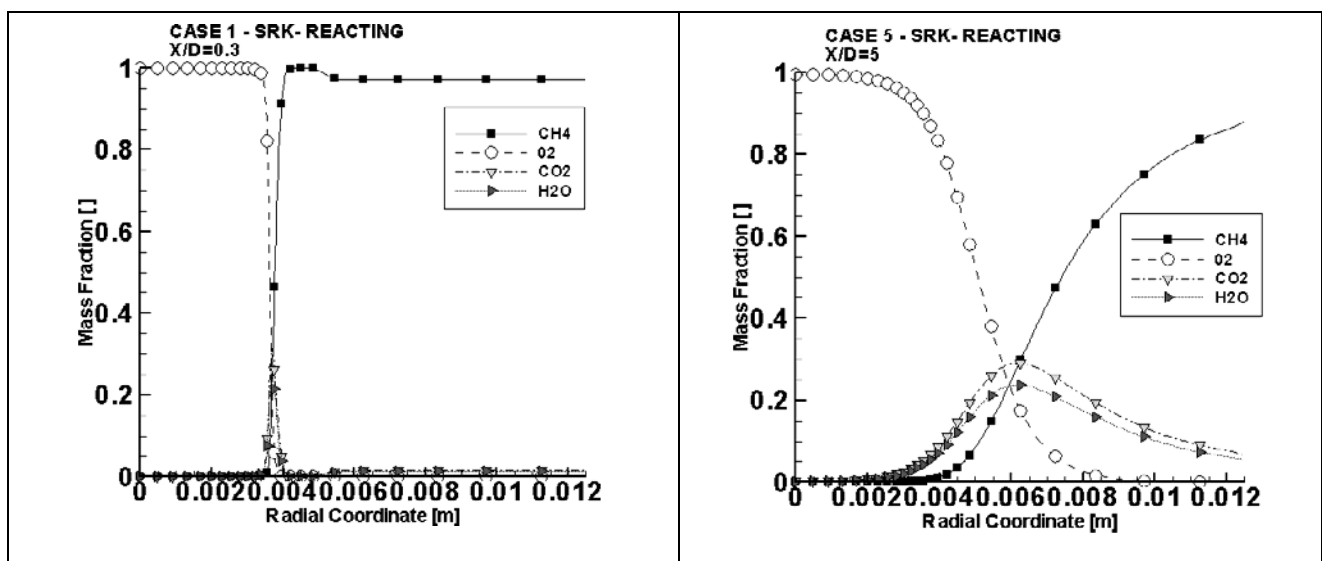


Figure 9 - Species radial profiles at $x/D=0.3$, and $x/D=5.0$ in the simulation with SRK equation of state.

5. Conclusions

This research has focused on a wide variety of issues related to modelling and basic studying high-pressure mixing and combustion processes in LO_x/CH₄ coaxial injector. Differences between ideal and real gas properties have been shown, by performing simulations by different approaches for the modelling of species properties: assuming ideal gas, using the NIST database and finally using two different real gas models, the Soave-Redlich-Kwong (SRK) real gas model and Peng-Robinson (PR) real gas model. Simulations show how real and ideal gas properties predict different species mass fractions and different jet potential core lengths. In particular, calculated values of the mixing length and species mass fraction profiles have been compared for the different models. While at supercritical temperature the agreement between the different approaches is quite good, when injection temperature is sub-critical, calculations by ideal gas and real gas equation of state give larger values of the mixing length than the simulation by the NIST database, showing a direct influence of the density ratio and isobaric specific heat. The modelling requires further comparisons with experimental data. Future studies will be also addressed to investigate the coupling between trans-critical injection and combustion and the use of a more accurate turbulence model.

References

- [1] W. Mayer, H. Tamura, "Propellant injection in a liquid oxygen/gaseous hydrogen rocket engine", *Journal of Propulsion and Power* 12 (6) (1996) pp. 1137–1147.
- [2] S. Candel, G. Herding, P. Scoufflaire, C. Rolon, L. Vingert, M. Habiballah, F. Grisch, M. Pealat, P. Bouchardy, D. Stepowsky, A. Cessou, P. Colin, "Experimental investigation of shear coaxial cryogenic jet flames", *Journal of Propulsion and Power* 14 (1998) pp. 826–834.
- [3] J. Smith, D. Klimenko, W. Clauss, W. Mayer, "Supercritical LOX/Hydrogen Rocket Combustion Investigations Using Optical Diagnostics", Paper AIAA-2002-4033, 38th AIAA/ASME/SAE/ASEE Joint Propulsion Conference & Exhibit, Indianapolis, 2002.
- [4] D. Chehroudi, Talley, and E. Coy, "Visual characteristics and initial growth rates of round cryogenic jets at subcritical and supercritical pressures," *Phys. Fluids* 14, pp. 850 (2002).
- [5] M. Oswald and A. Schik, "Supercritical nitrogen free jet investigated by spontaneous Raman scattering," *Exp. Fluids* 27, 497 (1999), 497–506.
- [6] B. Chehroudi, R. Cohn, D. Talley, and A. Badakhshan, "Cryogenic shear layers: Experiments and phenomenological modeling of the initial growth rate under subcritical and supercritical conditions," *Int. J. Heat Fluid Flow* 23, 554 (2002).
- [7] W. Mayer, R.J. Telaar, J. Branam, J. Hussong, "Raman measurements of cryogenic injection at supercritical pressure", *Heat and Mass Transfer* 39 (2003) 709–719.
- [8] M. Oswald, J.J. Smith, R. Branam, J. Hussong, A. Schik, B. Chehroudi, D. Talley, "Injection of supercritical fluids into supercritical environment", *Combustion Science and Technology* 178 (1–3) pp. 49–100, (2006).
- [9] J.C. Oefelein, V. and Yang, "Comprehensive Review of Liquid-Propellant Combustion Instabilities in F-1 Engines", *Journal of Propulsion and Power*, 9, 1993, pp. 657-677
- [10] V. Yang, "Modeling of Supercritical Vaporization, Mixing, and Combustion Processes in Liquid-Fueled Propulsion Systems", *Proceedings of the Combustion Institute*, 28, pp. 925-942, (2000).

- [11] J. C. Oefelein, and V. Yang, "Modeling high-pressure mixing and combustion processes in liquid rocket engines", *Journal of Propulsion and Power* 14, pp.843–857 (1998).
- [12] R.H. Augnier, A. Fast, "Accurate Real Gas Equation of State for Fluid Dynamics Analysis Applications", *Journal of Fluids Engineering*, 117, pp. 277-281, (1995).
- [13] M.R. Spiegel, J.M. Liu, "*Mathematical Handbook of Formulas and Tables, 2nd Edition*", The McGraw-Hill Companies Inc., pp 32-34, September 1968.
- [14] S. Gordon, B.J. McBride, M.J. Zehe, "NASA Glenn Coefficients for Calculating Thermodynamics Properties of Individual Species", *NASA TP-211556*, September 2002.
- [15] R.M. Pratt, "Thermodynamic Properties Involving Derivatives Using the Peng-Robinson Equation of State", *The National University of Malaysia – Chemical Engineering Education*, 2001.
- [16] S.M. Walas, "*Phase Equilibria in Chemical Engineering*", Butterworth-Heinemann, Boston, MA, 1985.
- [17] B. Carnahan, H.A. Luther, J.O. Wilkes, "*Applied Numerical Methods*", Wiley, New York, NY, 1969.
- [18] B.G. Kyle, "*Chemical and Process Thermodynamics*", Prentice Hall, NJ, 1994.
- [19] D. G. Friend, J. F. Ely and H. Ingham, "Thermophysical Properties of Methane," *Journal of Physical and Chemical Reference Data*, 18, No. 2, pp. 583–638, (1989).
- [20] R. Scmidt, and W. Wagner, "New Form of the Equation of State for Pure Substances and Its Application to Oxygen," *Fluid Phase Equilibria*, 19, No. 3, pp. 175–200, (1985).
- [21] N. Ierardo, A. Congiunti, C. Bruno, "Mixing and Combustion in Supercritical O₂/CH₄ Liquid Rocket Injectors", AIAA-2004-1163, 42nd AIAA Aerospace Sciences Meeting and Exhibit, Reno, Nevada, Jan. 5-8, 2004.
- [22] M. Oswald, F. Cuoco, B. Yang, M. De Rosa, "Atomization and Combustion in LOX/H₂- and LO_x/CH₄-Spray Flames", Institute of Space Propulsion, DLR Lampoldshausen, German Aerospace Center, 74239 Hardthausen, Germany.